Received: 31 October 2016 | Revised: 27 March 2017 | Accepted: 27 March 2017

DOI: 10.1111/vru.12524

IMAGING DIAGNOSIS

WILEY

Magnetic resonance imaging appearance of the brain and cervical spinal cord in an edema disease affected pig

Lucía Dieste-Pérez[1] | **Tetyda P. Dobak**[2] | **Federico R. Vilaplana Grosso**[3] | **Wilhelmina Bergmann**[4] | **Tijs J. Tobias**[1]

[1]Department of Farm Animal Health, Faculty of Veterinary Medicine, Utrecht University, Utrecht, Utrecht, The Netherlands

[2]Division of Diagnostic Imaging, Department of Clinical Sciences of Companion Animals, Faculty of Veterinary Medicine, Utrecht University, Utrecht, Utrecht, The Netherlands

[3]Department of Veterinary Clinical Sciences, Purdue University System, West Lafayette, IN, 47907

[4]Department of Pathobiology, Faculty of Veterinary Medicine, Utrecht University, Utrecht, Utrecht, The Netherlands

Correspondence
Lucía Dieste-Pérez, Department of Farm Animal Health, Faculty of Veterinary Medicine, Utrecht University, Utrecht, Utrecht, Netherlands.
Email: L.DiestePerez@uu.nl
Tijs J. Tobias, Department of Farm Animal Health, Faculty of Veterinary Medicine, Utrecht University, Utrecht, Utrecht, Netherlands.
Email: t.j.tobias@uu.nl

Abstract

A 7-week-old male pig was presented with signs of a central nervous system disorder. An MRI of the head and cervical spine was performed immediately after euthanasia. The MRI revealed multifocal bilaterally symmetric T2-weighted hyperintense lesions in the brain and spinal cord, likely due to a toxic metabolic process. Histopathological examination supported the MRI findings and confirmed the diagnosis of edema disease due to Shiga-like toxin produced by *Escherichia coli*. This is the first case published of the MRI findings in an edema disease affected pig.

KEYWORDS

central nervous system, MRI, Shiga-like toxin, swine, toxic metabolic disorder

1 | SIGNALMENT, HISTORY, AND CLINICAL FINDINGS

An approximately 7-week-old male Landrace × York cross-breed pig with clinical signs of a chronic and severe neurological disorder was presented for teaching purposes to the Farm Animal Health Clinic of the Faculty of Veterinary Medicine, Utrecht University, The Netherlands. Clinical examination was performed daily for three consecutive days. The pig suffered from anorexia and adipsia. It was severely growth retarded (10 kg BW) and stuporous. Breathing rate, rectal temperature, and heart rate were consistently slightly above the reference values. It showed an intermittent circling to the right and slight tremors over its body, and it often used its carpi for support. Examination of the nervous system showed no abnormalities of the cranial nerve reflexes. However, tactile and optic placement reflexes in the four limbs were delayed for 3 days. On the third day, the pig showed decreased responses in the hopping test and interdigital reflex in the hind limbs. The neurological signs worsened over 3 days and were indicative of a central nervous system (CNS) disorder. Due to the unspecific neurological signs, the lesion was suspected to be multifocal or diffuse, involving several areas of the central nervous system, potentially including the cerebral cortex, brain stem, cerebellum, and spinal cord. Differential diagnoses included infectious encephalomyelitis, metabolic or toxic encephalopathy, and, less likely, traumatic or congenital causes.

2 | IMAGING DIAGNOSIS AND OUTCOME

Due to the progression of the neurological signs and the poor prognosis, the pig was euthanized (Azaperone, IM 5 mg/kg BW, Elanco, Brussels, Belgium; and Pentobarbital sodium IC 150 mg/kg BW, Produlab Pharma B.V., Raamsdonksveer, the Netherlands). Shortly before euthanasia, an intravenous injection of contrast medium (Gadoterate meglumine, Guerbet, Aulnay-sous-Bois, France) was administered at a dose of 0.1 mmol/kg. The pig was placed in sternal recumbency, and MRI examinations of the brain and cervical spinal cord were performed in a 1.5 Tesla scanner (Philips Ingenia; Philips Medical Systems Nederland B.V., Best, the Netherlands) using a head coil. Images of the brain included postcontrast transverse T1-weighted spin echo (repetition time [TR] 694.2, echo time [TE] 14 ms, field of view [FOV] 130 × 138 mm, slice thickness 3 mm, matrix 276 × 198 mm); postcontrast T1-weighted 3D gradient echo (TR 20 ms, TE 4.6 ms, FOV

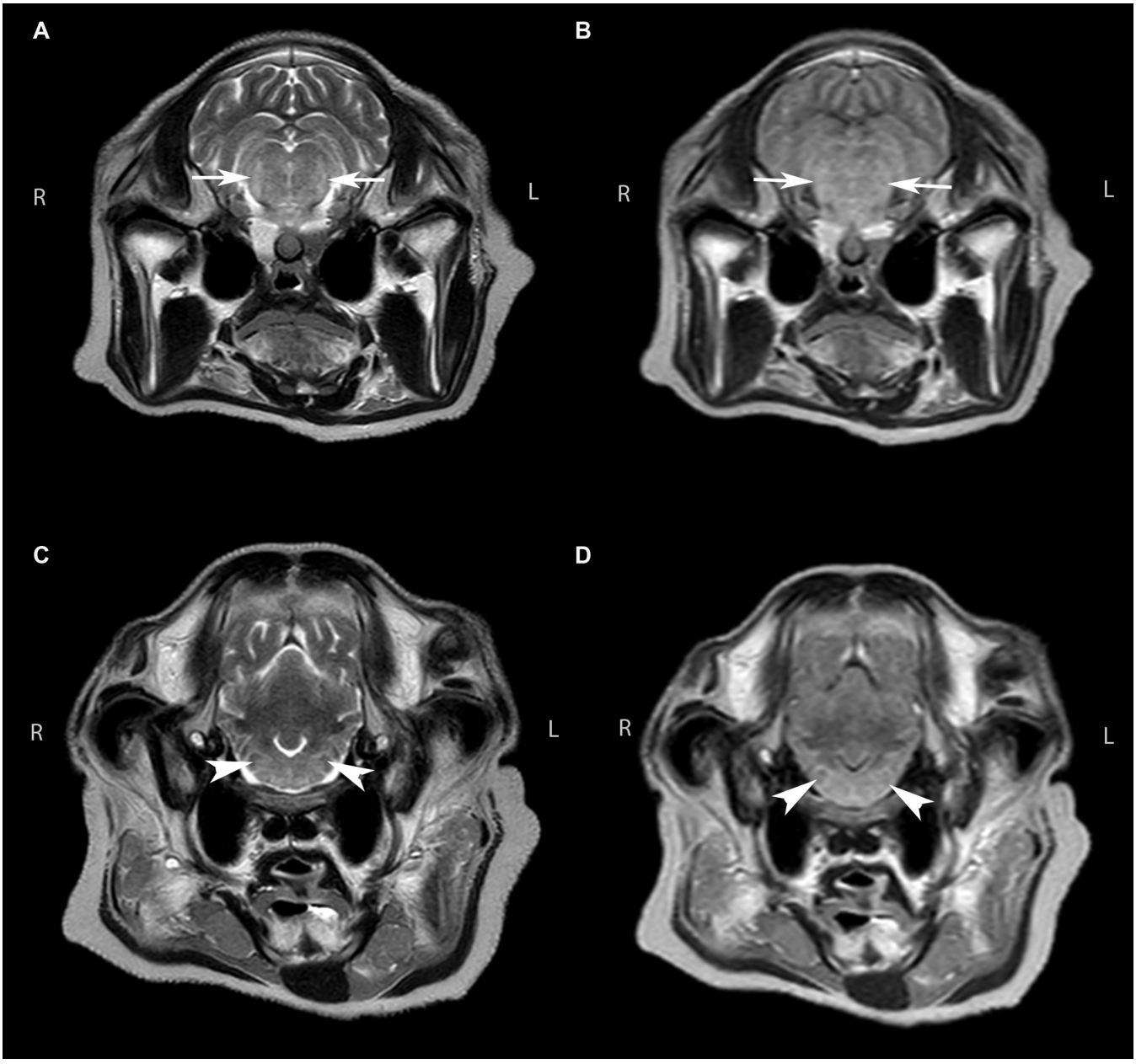

FIGURE 1 Transverse images at the level of the thalamus (A and B) and of the lingua of the cerebellum/medulla oblongata (C and D), including T2-weighted (A and C) and FLAIR images (B and D). Bilaterally symmetric, ill-defined T2 and FLAIR hyperintense lesions in comparison with the gray matter are seen affecting the thalamus (long arrow) and the medulla oblongata (arrowhead). L, left; R, right

130 × 130 mm, slice thickness 0.8–0.9 mm, matrix 164 × 164 mm) reconstructed in three planes; transverse T2-weighted turbo spin echo (TR 6013 ms, TE 100 ms, FOV 130 × 156 mm, slice thickness 3 mm, matrix 312 × 240 mm); transverse fluid-attenuated inversion recovery (FLAIR) (TR 11,000 ms, TE 140 ms, TI 2800, FOV 130 × 154 mm, slice thickness 3 mm, matrix 224 × 132 mm); and transverse T2* gradient echo (TR 852.4 ms, TE 13.8 ms, FOV 130 × 155 mm, slice thickness 3 mm, matrix 240 × 194 mm). Images of the cervical spinal cord included sagittal T1-weighted spin echo (TR 507.5 ms, TE 8 ms, FOV 160 × 248 mm, slice thickness 2.5 mm, matrix 239 × 312 mm); sagittal T2-weighted turbo spin echo (TR 2004 ms, TE 110 ms, FOV 160 × 248 mm, slice thickness 2.5 mm, matrix 228 × 312 mm); transverse T2-weighted turbo spin echo (TR 3000 ms, TE 110 ms, FOV 80 × 100 mm, slice thickness 2.4 mm, matrix 168 × 224 mm); and dorsal short-tau inversion recovery (STIR) (TR 5450 ms, TE 60 ms, TI 165 ms, FOV 200 × 250 mm, slice thickness 2.5 mm, matrix 201 × 280 mm) sequences. The interslice gap was 0.0 mm for all sequences.

Multifocal, intra-axial, extensive, bilaterally symmetric lesions were seen at the ventral aspect of both frontal lobes, involving gray and white matter, basal ganglia, corticospinal tracts, thalamus, hippocampus, and brain stem, including midbrain, pons, and medulla oblongata. Compared to the gray matter, the lesions were homogeneously T2-weighted and FLAIR hyperintense and T1-weighted isointense (Fig. 1). Lesions were also noted in the cervical spinal cord, involving the gray and white matter. The dorsal half of the spinal cord was diffusely, mildly heterogeneously T2-weighted and STIR hyperintense between

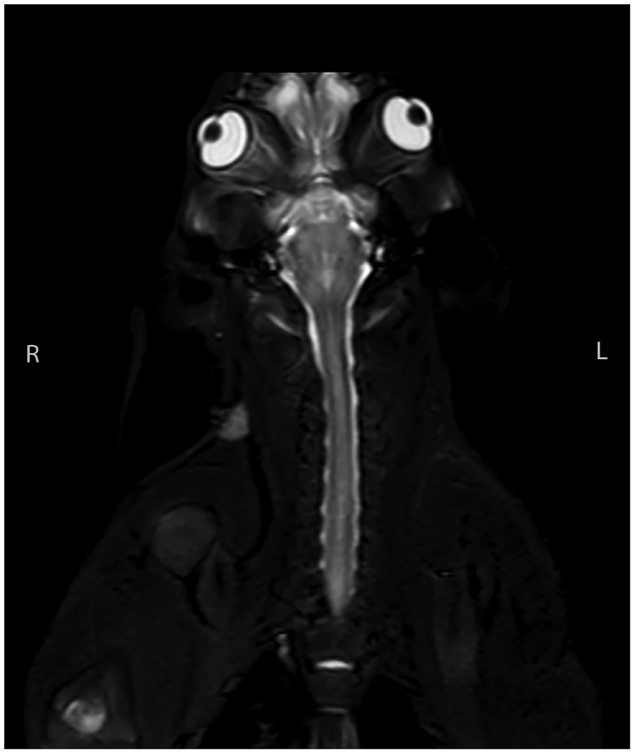

FIGURE 2 Dorsal STIR image of the brain stem and cranial cervical spinal cord. The medulla oblongata shows bilaterally symmetric, STIR hyperintense lesions when compared to the normal surrounding brain parenchyma. Similar lesions are also noted in the white and gray matter of the cranial cervical spinal cord

C1 and Th3 (Fig. 2). These lesions were T1-weighted isointense to very mildly hypointense. Despite the lack of precontrast T1-weighted images, no abnormal T1-weighted hyperintensities were noted, suggesting no contrast enhancement.

A toxic or metabolic cause was considered the primary differential for the bilaterally symmetric, T2-weighted hyperintense intracranial and intramedullary lesions. Directly after the MRI study, a cisternal cerebrospinal fluid sample was collected for analysis. Although the sample was contaminated with blood, cytology revealed no evidence of increased numbers of inflammatory cells.

Postmortem examination was delayed until 1 day after euthanasia due to logistic constraints. No macroscopic abnormalities of the brain or cervical spinal cord were identified and no evident edema in other tissues was observed. Histopathological examination of the central nervous system showed a multifocal acute fibrinonecrotizing vasculitis with moderate perivascular edema and malacia in the thalamus (Fig. 3), basal ganglia, hippocampus, and brain stem, a distinctive indicator of edema disease due to Shiga-like toxin produced by *Escherichia coli* (*E. coli*).[1] Unfortunately, isolation of *E. coli* could not be accomplished due to the decomposition stage of the intestines at the time of the postmortem examination.

3 | DISCUSSION

Inflammatory processes are the most common neurological disorders observed in pigs. At the farm level, euthanasia and postmortem

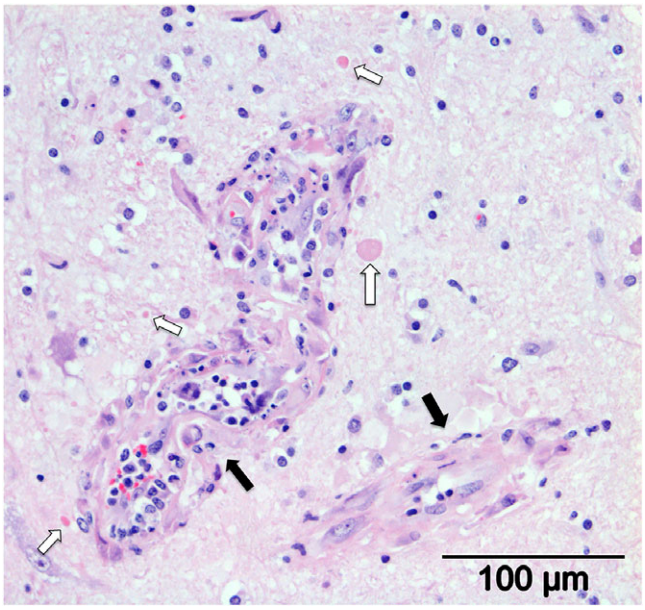

FIGURE 3 Histologic image of a section of the thalamus (H&E staining; 200× magnification). Fibronecrotizing vasculitis (black arrows) characterized by presence of macrophages and eosinophils (red granulae in the cytoplasm), swollen and necrotic endothelial cells, and perivascular edema (white arrows)

examination is usually the strategy chosen to ascertain the diagnosis. However, people have become more invested in animal welfare, and pet pigs are increasingly kept as companion animals. Therefore, in vivo tools are needed for a more accurate diagnostic approach in such cases. Analysis of the cerebrospinal fluid is one of the available tools to guide the diagnosis of central nervous system disorders. In addition to some practical constraints in pigs, there are limitations in this tool's ability to distinguish between inflammatory and noninflammatory processes.[2] The use of MRI in veterinary medicine has rapidly developed, and MRI is currently considered the test of choice for the diagnosis of neurological disorders.[3] However, literature about the use of diagnostic MRI in pigs is scarce. To our knowledge, this is the first published clinical report describing MRI findings in a pig affected by edema disease. Edema disease is a toxemia caused by the multiplication of some serotypes of *E. coli* in the intestine of pigs and the production of an angiotoxin called verotoxin 2e or Shiga-like toxin IIe after attachment to the intestinal villi.[4] Once absorbed in the intestine, the toxin reaches the target organs via the bloodstream, including the submucosa of many organs as well as the central nervous system. In these tissues, the toxin binds to the endothelial cells of small vessels, causing necrosis of smooth muscle cells, vascular leakage, and subsequent edema.[1,5] In recovered animals or chronic cases, edema cannot be clearly identified macroscopically, so histopathological examination is required to obtain the diagnosis.[5] In this case, it was difficult to localize the lesions within the central nervous system based on clinical signs only, and none of the in vivo laboratory tests under consideration helped to obtain a final diagnosis. Therefore, an MRI scan was performed.

The multifocal, bilaterally symmetric T2-weighted hyperintense lesions in the brain and spinal cord were compatible with edema,

malacia, necrosis, ischemia, or myelinolysis, among others.[6] Possible primary causes such as trauma, inflammation, or ischemic stroke were considered unlikely, due to the bilaterally symmetric distribution of the lesions.[3,6–9] This characteristic pattern has previously been described in cases of toxic metabolic diseases in small animals[6,10,11] and small ruminants.[2,12] In pigs, the most frequently found toxic metabolic disorders are hypoglycemia, salt intoxication, and edema disease.[13] To define a disease-specific lesion distribution in MRI could aid in guiding the differential diagnosis of a suspected toxic metabolic disorder. Hypoglycemia has been described in neonatal infants to follow an MRI pattern characterized by bilateral lesions mainly localized in the white matter of the parietal and occipital lobes,[14] although other areas such as the basal ganglia can be also affected, as reported in an insulinoma-affected dog.[15] The areas of the brain involved in hypernatremia-affected humans vary among patients, although the corpus callosum is a common localization.[16] In dogs, after correction of spontaneous hyponatremia the lesions seem to be predominantly restricted to the central thalamic nuclei.[17] Hemolytic uremic syndrome is a multisystemic disease in humans caused by a verotoxin produced by specific enterohemorrhagic strains of *E. coli*, with similar consequences in the brain as edema disease in pigs. In these cases, lesions observed in the MRI often involve the basal ganglia, but lesions in the thalamus, cerebellum, and brain stem have also been described.[18] In accordance with these studies, the multifocal, bilaterally symmetric lesions observed in this case were highly suggestive of a toxic metabolic disorder. The lesions in this pig seemed to be more extensive than in cases of hypoglycemia or hypernatremia, and the characteristic involvement of the basal ganglia in verotoxin toxemia was also present. However, additional studies are needed to identify a common pattern for edema disease.

Limitations of this study were that MRI was performed postmortem and that a precontrast T1-weighted sequence was not acquired due to logistical constraints. This sequence would be recommended for future clinical cases. Although MRI was performed within 30 min after euthanasia, authors acknowledge that there could have been some postmortem structural, chemical, or volumetric changes of the tissues, as well as other postmortem artifacts. Although more studies describing the MRI pattern of central nervous system disorders in pigs are necessary, authors believe that findings from this clinical case report support the use of MRI as a diagnostic test for pigs with suspected edema disease.

LIST OF AUTHOR CONTRIBUTIONS

Category 1

(a) Conception and Design: Dieste-Pérez L, Vilaplana Grosso FR, Tobias TJ

(b) Acquisition of Data: Dieste-Pérez L, Dobak TP, Bergmann W

(c) Analysis and Interpretation of Data: Dieste-Pérez L, Dobak TP, Vilaplana Grosso FR, Bergmann W

Category 2

(a) Drafting the Article: Dieste-Pérez L, Dobak TP

(b) Revising Article for Intellectual Content: Tobias TJ, Vilaplana Grosso FR, Bergmann W

Category 3

(a) Final Approval of the Completed Article: Dieste-Pérez L, Dobak TP, Vilaplana Grosso FR, Bergmann W, Tobias TJ

ACKNOWLEDGMENTS

Katja Bleeker is greatly acknowledged for her collaboration during the clinical examination of the pig and Ralph A. Edwards for proofreading.

REFERENCES

1. Gannon VP, Gyles CL, Wilcock BP. Effects of *Escherichia coli* Shiga-like toxins (verotoxins) in pigs. *Can J Vet Res*. 1989;53(3):306–312.
2. Schenk HC, Ganter M, Seehusen F, et al. Magnetic resonance imaging findings in metabolic and toxic disorders of 3 small ruminants. *J Vet Intern Med*. 2007;21:865–871.
3. Lamb CR, Croson PJ, Cappello R, Cherubini GB. Magnetic resonance imaging findings in 25 dogs with inflammatory cerebrospinal fluid. *Vet Radiol Ultrasound*. 2005;46(1):17–22.
4. Imberechts H, De Greve H, Lintermans P. The pathogenesis of edema disease in pigs. A review. *Vet Microbiol*. 1992;31:221–233.
5. Clugston RE, Nielsen NO, Smith DLT. Experimental edema disease of swine (*E. coli* enterotoxemia). III. Pathology and pathogenesis. *Can J Comp Med*. 1974;38:34–43.
6. Hecht S, Adams WH. MRI of brain disease in veterinary patients. Part 2: Acquired brain disorders. *Vet Clin North Am Small Anim Pract*. 2010;40(1):39–63.
7. Wessmann A, Chandler K, Garosi L. Ischaemic and haemorrhagic stroke in the dog. *Vet J*. 2009;180(3):290–303.
8. Incesu L, Khosla A. Imaging in bacterial meningitis. *Medscape*. 2015.
9. Yanai H, Tapia-Nieto R, Cherubini GB, Caine A. Results of magnetic resonance imaging performed within 48 hours after head trauma in dogs and association with outcome: 18 cases (2007–2012). *J Am Vet Med Assoc*. 2015;246(11):1222–1229.
10. Garosi LS, Dennis R, Platt SR, Corletto F, De Lahunta A, Jakobs C. Thiamine deficiency in a dog: Clinical, clinicopathologic, and magnetic resonance imaging findings. *J Vet Intern Med*. 2003;17:719–723.
11. Palus V, Penderis J, Jakovljevic S, Cherubini GB. Thiamine deficiency in a cat: Resolution of MRI abnormalities following thiamine supplementation. *J Feline Med Surg*. 2010;12(10):807–810.
12. Ertelt K, Oevermann A, Precht C, Lauper J, Henke D, Gorgas D. Magnetic resonance imaging findings in small ruminants with brain disease. *Vet Radiol Ultrasound*. 2016;57(2):162–169.
13. Dewey C. Diseases of the nervous and locomotor systems. In: Straw BE, D´Allaire SD, Mengeling WL, Taylor DJ, eds. *Diseases of Swine*. 8th ed. Ames, IA: Blackwell Publishing Ltd; 1999:861–882.
14. Barkovich AJ, Al Ali F, Rowley HA, Bass N. Imaging patterns of neonatal hypoglycemia. *Am J Neuroradiol*. 1998;19(3):523–528.
15. Fukazawa K, Kayanuma H, Kanai E, Sakata M, Shida T, Suganuma T. Insulinoma with basal ganglion involvement detected by magnetic resonance imaging in a dog. *J Vet Med Sci*. 2009;71(5):689–692.

16. Naik KR, Saroja AO. Seasonal postpartum hypernatremic encephalopathy with osmotic extrapontine myelinolysis and rhabdomyolysis. *J Neurol Sci*. 2010;291:5–11.
17. O'Brien DP, Kroll RA, Johnson GC, Covert SJ, Nelson MJ. Myelinolysis after correction of hyponatremia in two dogs. *J Vet Intern Med*. 1994;8(1):40–48.
18. Steinborn M, Leiz S, Rüdisser K, Griebel M, Harder T, Hahn H. CT and MRI in haemolytic uraemic syndrome with central nervous system involvement: Distribution of lesions and prognostic value of imaging findings. *Pediatr Radiol*. 2004;34:805–810.

How to cite this article: Dieste-Pérez L, Dobak TP, Vilaplana Grosso FR, Bergmann W, Tobias TJ. Magnetic resonance imaging appearance of the brain and cervical spinal cord in an edema disease affected pig. *Vet Radiol Ultrasound*. 2019;60:E15–E19. https://doi.org/10.1111/vru.12524